Special Feature: Advanced Thermal Management Technology for Developing the High-efficiency Vehicle

Research Report

A Development of Rapid and Uniform Thermal Cycling Test Technology for Electronic Components

Hajime Ikuno

Report received on Jun. 14, 2018

ABSTRACT A significant challenge in electronics is the reduction of solder joint thermal fatigue life spans. However, during testing, it can be difficult to both rapidly and uniformly cool or heat electronic device components due to the poor heat conduction exhibited by the materials in such components. The work reported herein developed a novel system for testing thermal fatigue based on the circulation of a shower of temperature-controlled air around specimens that allows rapid but uniform temperature control. Because the proposed apparatus permits multiple unit testing, a number of specimens can be examined simultaneously, thus increasing efficiency. The temperature profile of an actual electronic circuit board demonstrates that this system enables the target temperature to be attained rapidly, while providing a homogeneous temperature distribution. This new process reduces the thermal cycling period from 60 to 12 min but does not affect the extent of crack damage or the solder joint fracture mode.

KEYWORDS Electronic Component, Solder, Thermal Fatigue, New Test Method, Temperature Distribution

1. Introduction

A significant challenge in the field of electronics is the effect of thermal fatigue on solder joints. Thermal fatigue tests of metals are usually performed in cycles of a few minutes[1-6] and are used to improve the reliability of engine parts, materials, etc. Conversely, the thermal assessment of components of electronic devices generally applies cycle times in excess of one hour.[7,8] These prolonged cycling durations are necessary due to the low heat conductivity of the ceramics, resins and other materials in such devices, which result in unique distributions of strain and temperature in response to fast cooling or heating. Moreover, the fracture mode may change because the ceramics used in these components have low fracture toughness and therefore fracture easily due to thermal shock.

In order to shorten the test time for such electronic components, a new technology that enables all of the low-thermal-conductivity materials of electronic components to be heated and cooled uniformly and rapidly must be developed.

A test performed in the liquid phase[9] exists that is able to quickly determine the ability of electronic components to resist thermal fatigue, although the associated heating and cooling (H/C) rates are many times higher than those that might be encountered in actual use.[9,10] In this paper, we designed a new technique that incorporates fast H/C but is similar to the existing gas-phase tests. A simple yet efficient test system capable of simultaneously assessing multiple units was also developed.

2. Conventional System and Associated Challenges

A schematic diagram of the conventional thermal cycle test system is shown in **Fig. 1**. This apparatus utilizes air circulation to perform gas-phase tests.[11-13] The system consists of three chambers: a test chamber (into which test specimens are placed), a hot chamber that generates high-temperature air, and a cold chamber that generates low-temperature air.[11,12]

During heating, hot air is rapidly injected into the test chamber in order to quickly heat the sample. During cooling, precooled air is injected to rapidly cool the sample in the same manner. However, although the temperature distribution of the samples

in the test chamber is relatively uniform because of the slow heat transfer through the air, the temperature control response is not as fast because of the large heat capacity of the chamber.

As noted, in order to increase the rate of the chamber temperature change, preheated or precooled air is rapidly injected into the test chamber, although the temperature change rate may vary significantly based on variations in the sample position in the chamber. In addition, although multiple samples can be tested simultaneously in one chamber, the H/C rate may vary widely due to the total heat capacities of different samples.

As indicated by the temperature profile in Fig. 1, the air temperature changes rapidly during the initial stages of heating or cooling and then begins to vary more slowly as the high or low target temperature is approached. Since the sample temperature changes more slowly than the air temperature, the sample approaches the target temperature more slowly, so the thermal cycle period must be extended to approximately 60 min.

3. Features of the Proposed System

3. 1 Basic Concept

Herein, we present the basic concept of the proposed system. Because the heat capacity per unit volume of air is generally less than that of a solid or liquid, the heat transfer from the air to the sample is poor when the air is blown directly onto the surface of the sample. As such, the temperature of the sample surface changes slowly. This slow temperature change of the sample surface prevents the formation of a significant temperature difference between the surface and inner part of the sample during H/C.

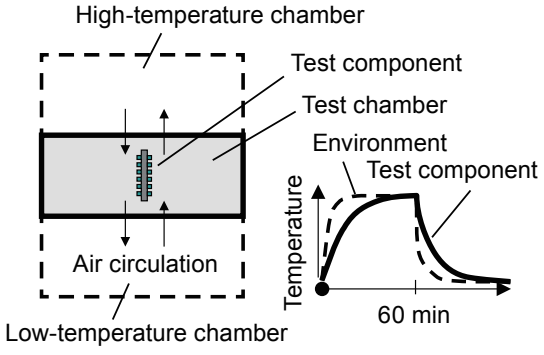

Fig. 1 Conventional thermal cycling test system.

In a conventional test unit, slow H/C to the actual target environment can be achieved by this mechanism. Thus, the gas-phase H/C mechanism is important in terms of preventing an increase in the temperature difference between the surface and the inner part of the sample. This basic concept is also incorporated into the proposed system. However, using the current method, the temperature distribution over a large sample will be somewhat uneven because some parts of the sample are in contact with the incoming hot or cold air whereas others are not. Moreover, in the case of a sample having a large thermal capacity, significant time is required to realize a uniform temperature distribution over the surface by means of heat conduction. Therefore, a rapid temperature change may generate an unwanted temperature distribution throughout the sample.

To address these problems, air must be uniformly blown onto all parts of the samples, and the optimal means of doing so was investigated in the present study. Furthermore, the air temperature is changed as a result of heat transfer when the air touches the samples, so the temperature change at the first point at which the incoming air makes contact will be more rapid. In contrast, the temperature change will be slower at the downstream part of the sample, which can cause large temperature differences at different positions. Both rapid air circulation and quick control of the temperature are needed in order to address this problem and to reduce the temperature difference between the upstream and downstream air.

3. 2 Basic Structure of the Proposed System

The basic structure of the proposed system is shown in **Fig. 2**. This apparatus uses a new mechanism termed a temperature-controlled air-shower circulation system to blow air uniformly over the entirety of large electronic components. The mechanism by which this system operates is described below.

Initially, either room temperature or low-temperature compressed air is provided. The temperature of the air can be rapidly modified via a heating unit. The air is ejected and dispersed as a shower into the test chamber from small holes in the nozzle of a supply pipe attached to the outlet of the air heater. Test samples such as large circuit boards are placed in the center of the test chamber, and the air shower circulates air around the test samples, providing uniform heat transfer to all

parts. This system enables both rapid and uniform H/C using only a small amount of air.

The test chamber incorporates uniformly distributed slit-shaped exhaust ports and optimally positioned inlet nozzles and outlet ports to enable uniform airflow. Furthermore, the inner chamber walls are insulating, and thus allow the heat of the incoming air to be efficiently transferred to the test samples without heat loss.

The chamber air temperature, which is measured using a temperature sensor placed in the chamber, is controlled at the target temperature by adjusting the output of the air heater. Because the entire chamber can be uniformly heated and cooled, simply controlling the chamber air temperature allows the sample temperature to be adjusted. Therefore, uniform and rapid H/C of the test samples is possible without attaching temperature sensors to the test samples. In contrast to the conventional system, in which the overall airflow in the chamber is generated by a fan, the proposed system injects a high speed air shower from the nozzle, resulting in rapid air circulation. Moreover, the air is quickly discharged from the chamber after the temperature is changed by circulation. Accordingly, because temperature-controlled air is constantly circulating, the temperature difference among the sample positions is extremely small.

As the air temperature is controlled with both high responsivity and high accuracy, this newly developed system provides rapid H/C of all parts of the sample. Even when the temperature of the air is changed rapidly, because heat is transferred uniformly and quickly over the sample, the entire specimen can be speedily heated or cooled while maintaining a uniform temperature distribution.

3.3 Visualization of the Airflow in the Chamber

The geometric model used to visualize the airflow in the test chamber by computational fluid dynamics (CFD) is presented in **Fig. 3**. The inner dimensions of the test chamber in this model are 210 × 210 × 80 mm and a test sample having dimensions of 180 × 190 × 30 mm is placed in the center of the chamber. The dimensions of the air nozzle and the outlet slits are as shown in Fig. 2. The ANSYS CFX software package was used for the CFD analysis.

Layered meshes were placed at the surface boundary between the fluid air and the solid wall in order to take into account the influence of the hydrodynamic boundary layer. The meshes near the air nozzle were fine and became coarser farther from the nozzle, reflecting the actual tendency of the distribution of the airflow rate. Tetragonal meshes were used due to the complexity of the model. The number of elements was approximately one million.

Figure 4 shows the airflow in the test chamber as visualized by the CFD analysis. The air showers ejected from the nozzles flow through the upper region above the sample before striking the wall opposite and returning through the lower region below the sample. The air is subsequently discharged from the outlet. This figure confirms that the airflow is approximately the same as that shown in Fig. 2.

3. 4 Construction of a Multi-unit System

We also developed a multi-unit system consisting of a number of rapid uniform test units, enabling the simultaneous evaluation of numerous test samples. **Figure 5** shows the system configuration. In this

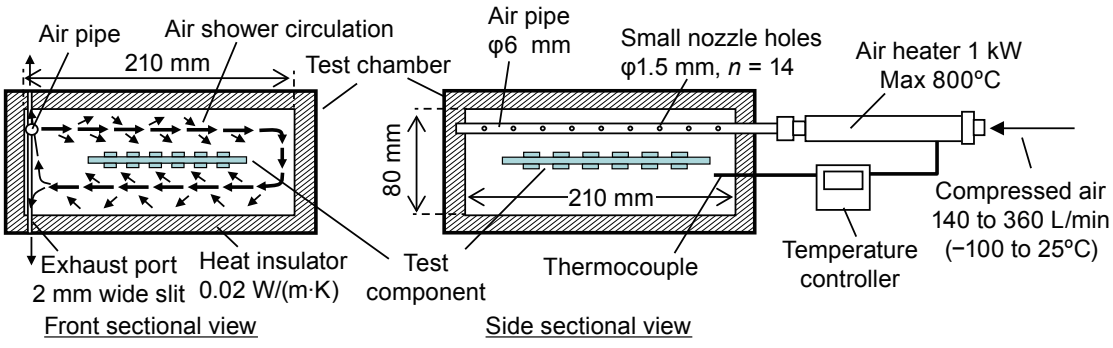

Fig. 2 Schematic diagram of the basic structure of the proposed system.

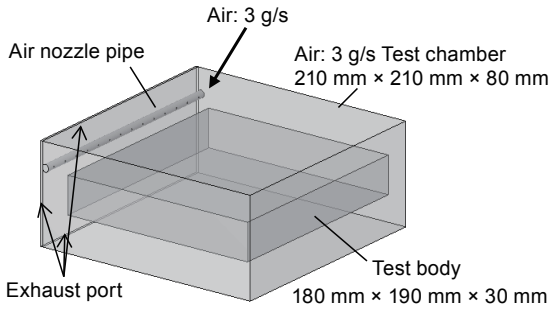

Fig. 3 Geometry model for analyzing airflow in the test chamber of the proposed system.

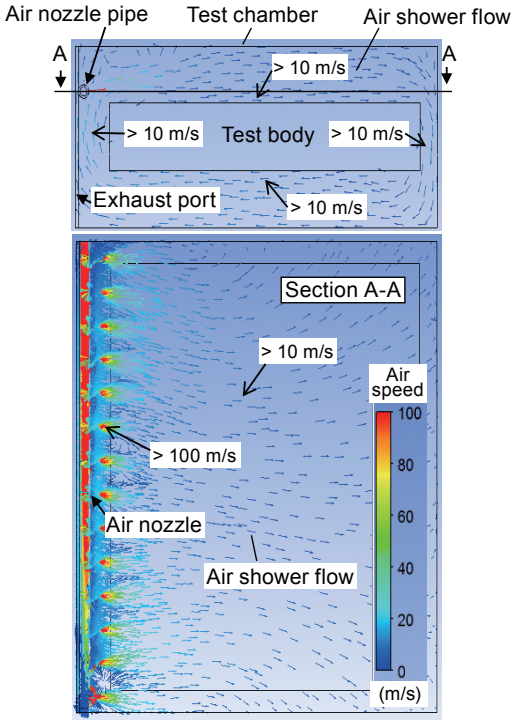

Fig. 4 Air flow visualization by CFD analysis in the test chamber of the proposed system.

apparatus, ambient and low-temperature compressed air pipes are branched and connected to the multiple test units through solenoid valves. The combination of airflow path selection and rapid air temperature control via a heater enables thermal cycling over a wide temperature range and a wide range of H/C rates. As an example, room temperature air can be heated, while the low-temperature air cooled by a refrigerator is also controlled with the support of the air heater. In both cases, the final temperature achieved using the air heater is accurate and is reached rapidly.

All controls in this system are based on a multi-task program run on a personal computer. As such, each unit can be operated under independent conditions, and tests can be started and stopped independently without affecting the operations of the other test units.

4. Results and Discussion

4. 1 Temperature Profiles of Air in Chambers without Samples

The air temperature profiles in the test chambers of the two systems were compared without samples. The conventional system was a TSV-40HT-W (Espec Corp.), with test chamber dimensions of 390 mm (width) × 320 mm (height) × 460 mm (depth). The specifications of the proposed system are as shown in Fig. 2, with chamber inner dimensions of 210 mm (width) × 210 mm (depth) × 80 mm (height).

The test results are summarized in **Fig. 6**. In the conventional system, the temperature change rate is high during the initial stage of heating and then gradually decreases as the high target temperature

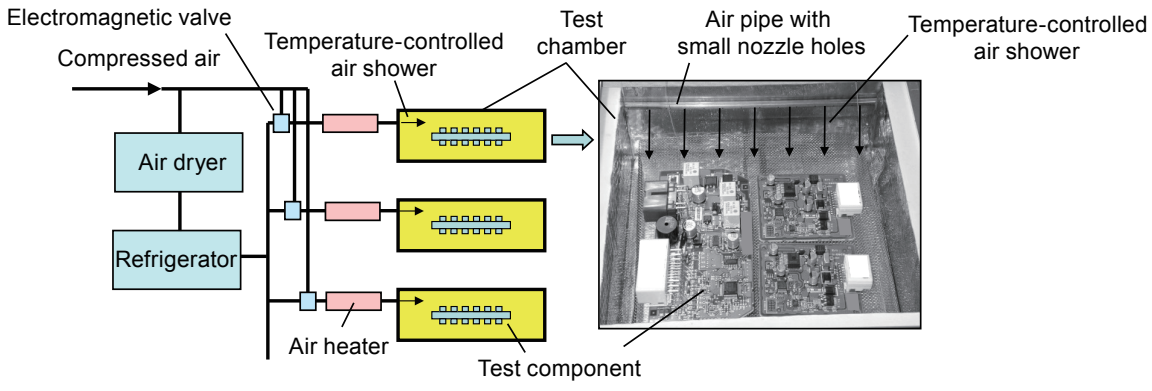

Fig. 5 Schematic illustration of the developed multi-unit system.

is approached. In addition, temperature overshoot is observed just after reaching the high target temperature. In contrast, the temperature change rate of the proposed system is lower than that of the conventional system during the initial stage of heating. However, the heating time required for the proposed system to reach the high target temperature is shorter than that for the conventional system, because the temperature change rate remains approximately constant until the target temperature is approached. The new unit did not exhibit temperature overshoot after reaching the target temperature because the temperature was quickly controlled at a constant value.

Similarly, in the new system, despite the low cooling rate during the initial stage of cooling, the time required to approach the low target temperature is shortened due to the small reduction in the cooling rate until the low target temperature is approached. In the soaking stage following cooling, the temperature is also held constant without overshoot. However, in the conventional system, overshoot below the low target temperature of 30ºC occurs due to the slow temperature control response.

As discussed, despite the slow H/C rate during the initial stage in the newly developed unit, the time required to reach the target temperature is shortened as a result of the minimal reduction in the temperature change rate until the target temperature is approached. In addition, the temperature was found to be constant during soaking after H/C, evidently as a result of the rapid temperature control response.

If the temperature change rate is too high, the temperature distribution in the test samples may become significant, yielding results that differ from those obtained under practical use conditions. Because the temperature change rate and the thermal uniformity generally have a trade-off relationship, the proposed system offers superior thermal uniformity due to the reduction in the maximum temperature change rate during the initial stages of H/C. This effect results

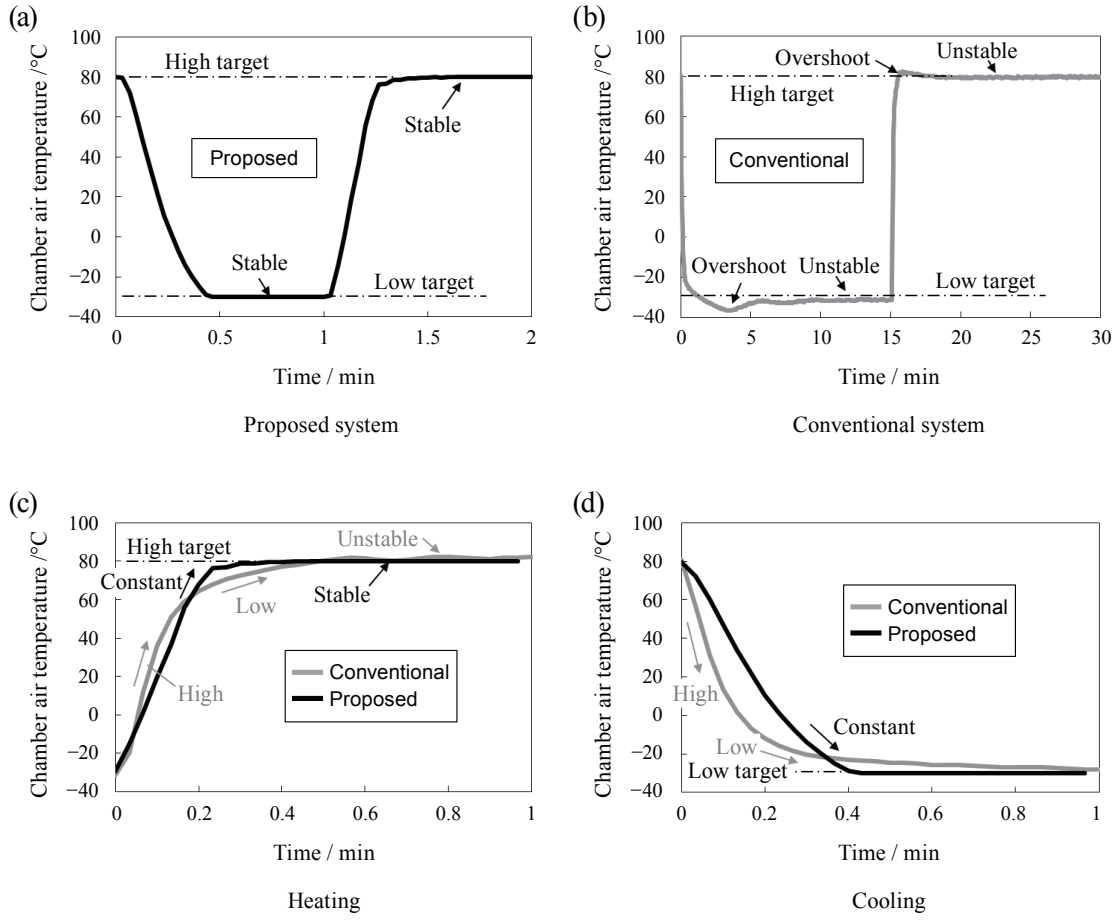

Fig. 6 Temperature profiles of air in the empty test chamber (no test sample).

from the temperature-controlled air-shower circulation system, which permits both rapid and uniform H/C using a small amount of air.

4. 2 Temperature Profiles in Test Chambers with a Test Component

Figure 7 shows the test component examined in the present study, having outer dimensions of 175 × 165 × 25 mm and a mass of 197 g. This specimen was selected as a representative example of a large, heavy circuit board with numerous relatively large mounted electronic parts. In this figure, points "a" through "d" indicate the positions at which thermocouples were attached for the purpose of temperature measurement. The thermal cycling test systems used to evaluate this sample were as described in Sec. 4. 1. The test component was placed approximately in the center of the test chamber of each system.

The temperature profiles acquired at various parts of the sample are provided in **Fig. 8**. The upper, middle and lower rows of figures comprise the complete thermal cycle curves and close-ups of the curves near the high and low target temperatures, respectively,

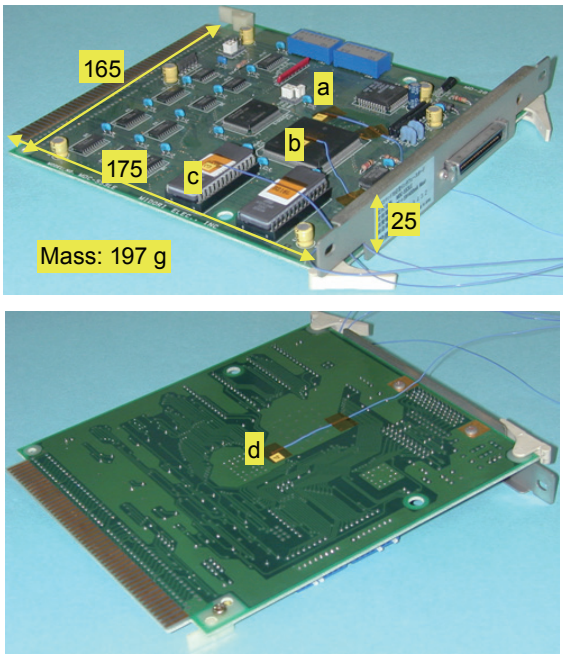

Fig. 7 Photographs of the electronic component evaluated in the temperature distribution tests. "a" through "d" indicate temperature measurement points, at which thermocouples are attached.

for the proposed (left) and conventional (right) systems. The H/C rate and the temperature control performance can be determined using these figures. The cooling curves shown in Figs. 8(b1) and (b2) indicate that the time required for the proposed system to reach the target temperature was less than that for the conventional unit. Furthermore, in the proposed system, the temperature was maintained at a constant value after reaching the target temperature. In contrast, in the conventional system, the temperature overshot the target temperature.

Similarly, the heating curves in Figs. 8(c1) and (c2) demonstrate that the target temperature was reached sooner using the proposed system. In addition, in the case of the newly developed unit, the temperature remained constant after reaching the target value. In the conventional system, although the chamber rapidly approached to within a few degrees Celsius of the target, the desired temperature was not actually reached.

The temperature change during soaking using the conventional system is summarized in **Fig. 9**. Based on the heating curve in Fig. 9(a), the target temperature was gradually approached over the course of several tens of minutes. The same behavior is observed in the cooling curve in Fig. 9(b). Furthermore, during both temperature change directions, the curves oscillate near the target temperature, which suggests that the control performance was unstable. In contrast, the proposed system maintained the temperature at a constant value during soaking in a stable manner, as demonstrated in Figs. 8(b1) and (c1). As described above, the proposed system approached the target temperature faster than the conventional system and also exhibited more stable control performance during soaking after reaching the target. The temperature profiles at the various parts of the test sample upon cooling are provided in **Fig. 10**. Figures 10(a1) and (a2) show the results for cooling using the proposed and conventional units, respectively, while Figs. 10(b1) and (b2) present data for heating using the two units. The former two figures show that the temperature distribution among the sample positions obtained using the proposed system were generally slightly narrower than that generated with the conventional system.

As shown in Fig. 10(a2), for the conventional system, the cooling rate during the initial stage of cooling was high, after which the temperature distribution broadened. In contrast, an initial quick temperature

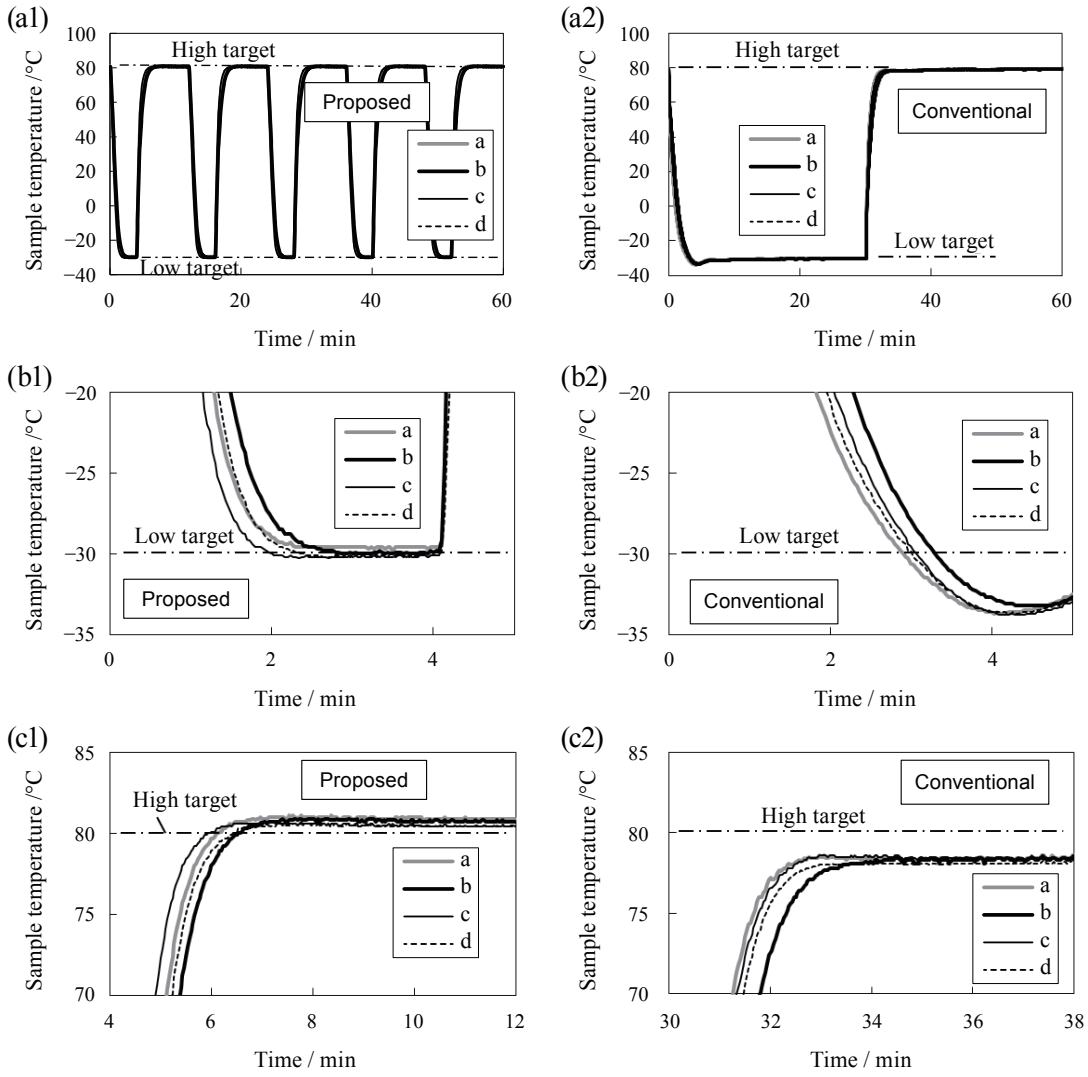

Fig. 8 Temperature profiles obtained for the test component.

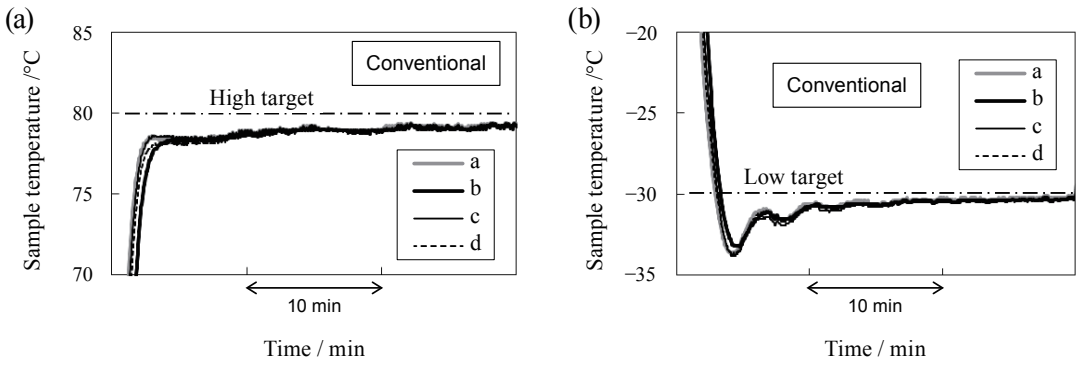

Close-up of the temperature distribution near the low target temperature (conventional system)

Close-up of the temperature distribution near the high target temperature (conventional system)

Fig. 9 Temperature profiles near the high and low target temperatures for the conventional apparatus.

change was not observed when using the proposed system, but rather the temperature distribution changed gradually (that is, the distribution expanded slowly during cooling and contracted upon approaching the target temperature). Furthermore, the temperature difference between closely situated sample positions "a" and "b" was smaller for the new unit than for the conventional system.

Similarly, in the heating curves shown in Figs. 10(b1) and (b2), the proposed system exhibits normal behavior, meaning that the temperature distribution gradually increases during heating and then decreases as the target temperature is approached. In contrast, for the conventional system (similar to the behavior observed during heating), the temperature changed rapidly during the initial stage, resulting in a broader temperature distribution among the sample positions. Moreover, the temperature difference between closely situated positions "a" and "b", which was large for the conventional system, was small for the proposed system. Although the time at which the maximum temperature difference among the positions of the sample occurred differed according to the system, this difference tended to be always be smaller for the new apparatus.

The differences in the temperature distribution described above are considered to result from variations in the thermal cycling methods employed. In the conventional system, air having a significantly different temperature from ambient is abruptly supplied to the test chamber, so the temperature changes rapidly during the initial stages of H/C. This scenario tends to result in large temperature differences among the individual positions on the sample. In the proposed system, a smaller amount of air is uniformly dispersed and then circulated around the sample, so the temperatures of all positions of the sample change similarly and simultaneously, resulting in a small temperature difference. Therefore, as noted, the new technique provides a more uniform temperature distribution than the conventional system, despite the rapid H/C rate.

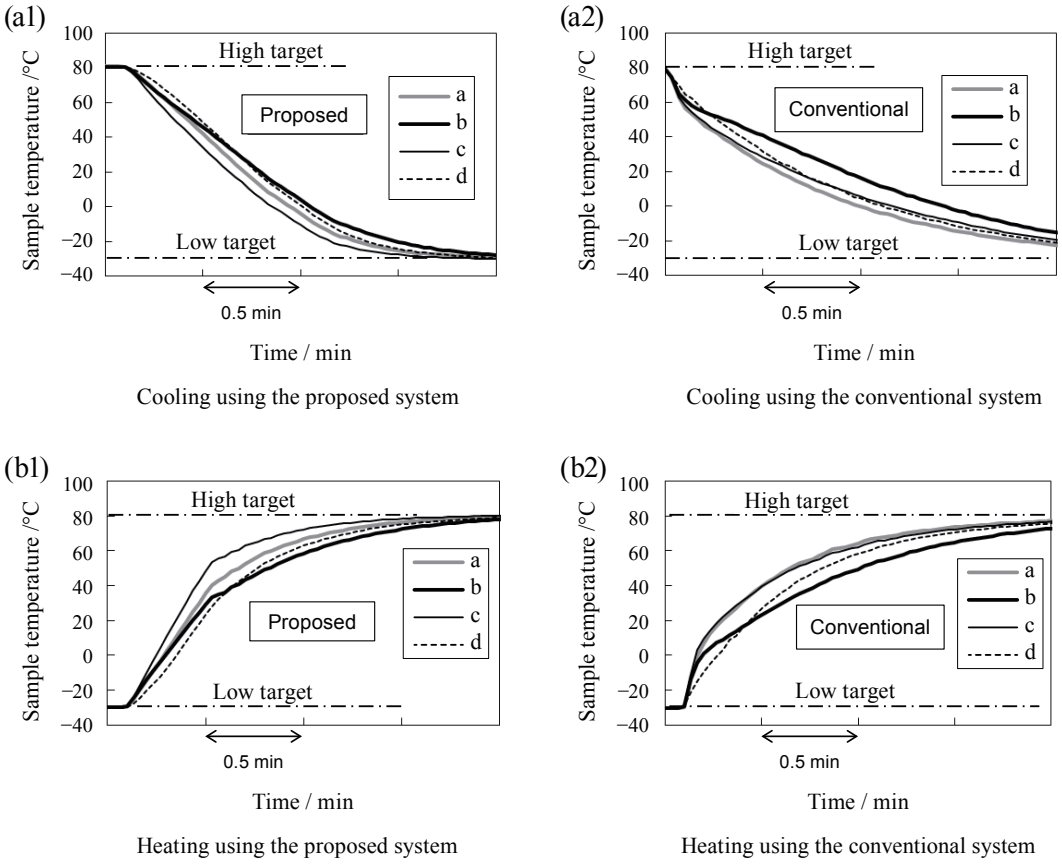

Fig. 10 Temperature distributions obtained using the proposed and conventional systems.

Finally, the temperature profiles of the chamber air and the representative sample positions obtained using the proposed and conventional systems were compared with a sample component in the test chamber. In the conventional system, the temperature difference is greatly affected by the specific region of the chamber in which the sample is located, as the air temperature is measured at the chamber center near the sample. In the proposed system, however, the airflow in the chamber is uniform, so temperature variations throughout the chamber are reduced, and the air temperature is measured near the chamber wall.

The air temperature profiles in the test chambers are shown in **Fig. 11**. Figures 11(a) and (b) present the respective temperature profiles of the new and existing systems during the initial stages of H/C. The heating curves shown in Fig. 11(a) indicate that, in the case of the conventional system, the temperature changed rapidly during the initial stage and then slowly approached the target temperature. Although the rate of temperature change during the initial stage was low in the case of the proposed system, the temperature reached the desired value earlier because the decrease in the rate of change was small until very near the target temperature.

The cooling behavior tended to mimic the heating behavior in that, for the proposed system, the temperature changed rapidly until close to the target temperature, which was reached earlier compared to the conventional system. The time required to achieve the target temperature was longer for the test chamber with a sample present than without a sample (Fig. 7). However, the temperature change behaviors were similar.

Based on the above results, in the proposed system, the chamber air temperature is controlled to maintain the change rate approximately constant until the target temperature is approached. This behavior appears to decrease the time required to reach the target temperature. In the conventional unit, the temperature changes rapidly during the initial stage. However, the temperature control near the target is slow and unstable, which has been found to increase the testing time. The use of a reduced air flow with a uniform distribution around the sample to quickly control the temperature in the proposed system is considered to enable rapid and uniform thermal cycling. The conventional system consists of thermostatic chambers with air circulation and, as such, the response of the temperature control is generally slow due to the high heat capacity of these chambers.

Even if the chamber temperature is increased by pre-heating or via a hot airflow in an attempt to increase the heating rate, the temperature increases rapidly during the initial stage but the heating rate decreases as the target temperature is approached. Thus, reaching the high target temperature takes a long time. In addition, increasing the heating rate may broaden the temperature distribution of the sample, causing the test results to differ from those under practical use conditions.

In the proposed system, the heat capacity is low due to the simple structure of the chamber and the control response of the air temperature provided by blowing heated air from outside the chamber is significantly faster. Thus even though the temperature change rate

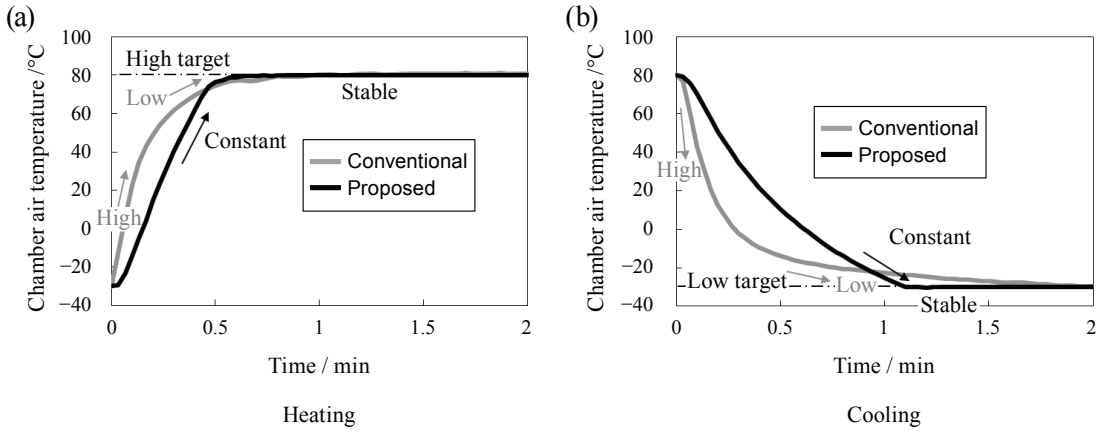

Fig. 11 Temperature profiles of the air in the test chamber containing the test component.

during the initial stages of H/C is lower than that for the conventional system, the time required to reach the target temperature is shorter as a result of the effectiveness of the temperature control mechanism.

4. 3 Effects of Thermal Cycle Period on Solder Joint Damage

The effect of the more rapid thermal cycling using the proposed system on solder joint damage was examined. The test sample considered in the present study is shown in **Fig. 12**. This specimen was an FR4 circuit board having R3216 chip resistors mounted on both sides by solder joints. The chemical composition of the solder, which was a typical lead-free material, was Sn-3Ag-0.5Cu (wt%).

Soldering was performed using a commercially-available reflow furnace. The reflow temperature conditions were as recommended by the solder manufacturer (peak temperature: 230 to 255ºC, hold time above 220ºC: 30 to 60 s). The chip resistors were commercially available 0-ohm resistors. The evaluation results indicated that the resistance of the unit increased in conjunction with crack propagation in the solder joints. The number of cycles to failure was determined by identifying the point at which the rate of change in resistance exceeded a predetermined value.[14,15] In the present study, the change in resistance between the ends of solder joints was precisely measured by a four-terminal method using a milliohm meter in order to evaluate the amount of crack propagation. A total of 24 chip resistors were mounted on both sides of the circuit board, as shown in Fig. 12. The changes in resistance were measured for all joints and the damage was evaluated based on the statistical values of these results.

Thermal cycling tests were conducted using the proposed system. We considered two test profiles: a rapid profile consisting of heating for 8 min and cooling for 4 min (cycle period: 12 min), and a conventional profile consisting of heating for 30 min and cooling for 30 min (cycle period: 60 min). The test temperature range for each condition was from −30 to 80ºC, and the time required for the test sample to reach the target temperature was within 2 min for both heating and cooling.

The resistance changes in the joints during 3000 thermal cycles are shown in **Fig. 13** for the two abovementioned test profiles. The circles indicate the mean values for 24 joints, and the error bars indicate standard deviations. These statistical values were used to compare the two sets of results because

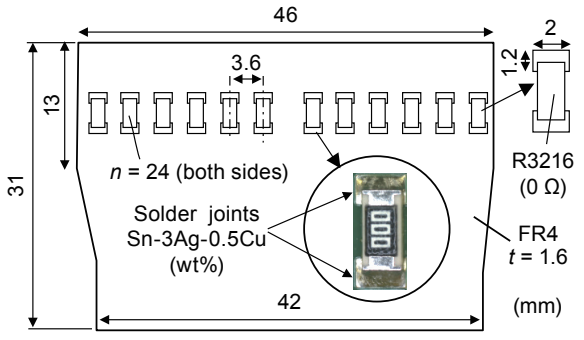

Fig. 12 Sample test component used to evaluate thermal fatigue damage in solder joints.

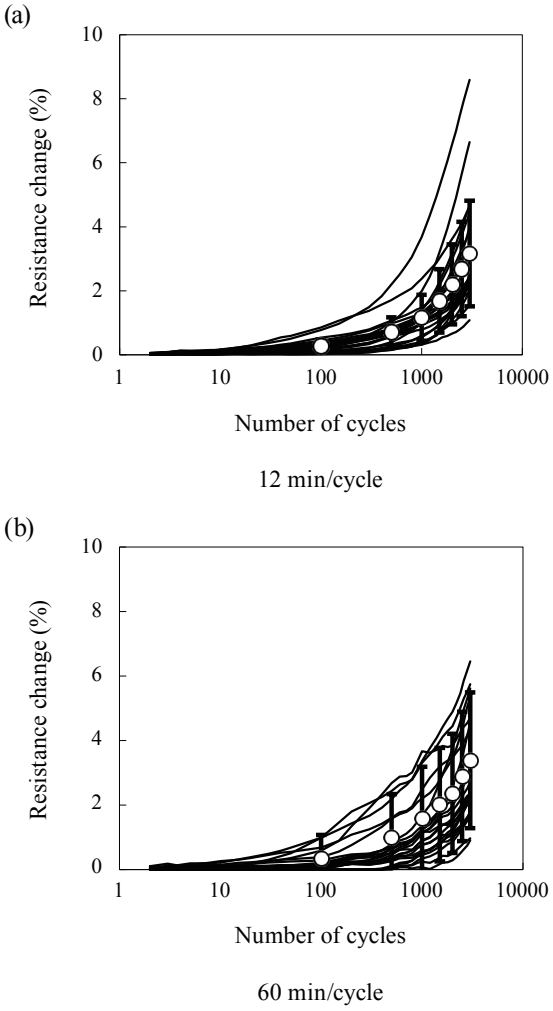

Fig. 13 Resistance changes of solder joints during 3000 cycles (−30ºC↔80ºC).

the resistance changes varied widely between the joints. The data confirm that the resistance changes were similar for both test profiles (12 min/cycle and 60 min/cycle). The cross-sections of solder joints after 3000 thermal cycles are presented in **Fig. 14**. Crack propagations in the solder joints under the chips was observed to be similar for both conditions.

The thermal cycle testing of electronic components is a standard method for evaluating durability under practical use conditions within a short time span.[10] It has been reported that tests that are performed too rapidly (at a temperature change rate of several tens of degrees Celsius per second, meaning thermal shock tests)[9] can induce a fracture mode that is different from that which occurs during normal thermal cycling tests. Therefore, thermal cycling tests are performed slowly in the gas phase. In addition, the soak times during the high- and low-temperature periods are defined such that the minimum soaking time is 1 min. In order to take into account creep due to soldering fatigue, for example, the soaking time is recommended to be greater than 5 min.

The conventional system[14,16-18] complies with this thermal cycling test standard and is widely used for accelerated testing to evaluate durability under market (that is, practical use) conditions. Because the proposed system can also be used for the same type of testing in the gas phase and provides a more uniform temperature distribution than the conventional unit, this new method also complies with the standard but can be used for faster evaluation. Furthermore, the soaking time for the proposed system also complies with the standard.

Here we explain why the test results for both test conditions were similar. In both cases, the temperature change rates during the heating and cooling periods were the same, so the only difference was in the soaking times at the high and low target temperatures. A long soaking time may affect the thermal fatigue damage. Generally, the creep behavior of metallic materials consists of primary creep (in which the strain rate decreases with soaking time), secondary creep (in which the strain rate is constant) and tertiary creep (in which the strain rate increases with time, leading to rupture).[19] In case of the solder used in this study, the time range over which primary creep occurred was several minutes and the secondary creep strain rate was less than that of the primary creep.[20]

Conversely, since the thermal fatigue of solder joints occurs due to differences in the thermal expansion coefficients of the constituent materials, the stress relaxes during the soaking time. In addition, the creep rate is strongly affected by the stress level, and thus stress relaxation yields a remarkably lower rate of creep strain.

For these reasons, the creep strain in the current work was predicted to increase rapidly during the initial few minutes of the test and then to decrease immediately afterwards as a result of stress relaxation. That is, after the initial several minutes of soaking time, the strain change was anticipated to be minimal. In this study, the soaking times at the high target temperatures (at which the creep effect occurs) were longer than several minutes, and therefore the creep strain levels were equal for both test conditions, resulting in the observed similar degree of thermal fatigue damage. The limitation on soaking time in the temperature cycling test standard is considered to take these behaviors into account.

The proposed system satisfies the basic requirements of the thermal cycling test, so the damage state was reproduced even when the test period was reduced, as described above. With regard to the high-temperature soaking time, because creep behavior can result in more significant damage[21] due to the restrained state of the sample, the acceleration ratio and the most suitable test conditions should be considered. In addition, in the case that the temperature difference between the surface and the inner part of the samples is important, the H/C rates should be adjusted accordingly. The proposed system provides rapid temperature control performance, so suitable test conditions can be realized by freely adjusting both the H/C rates and the soaking time.

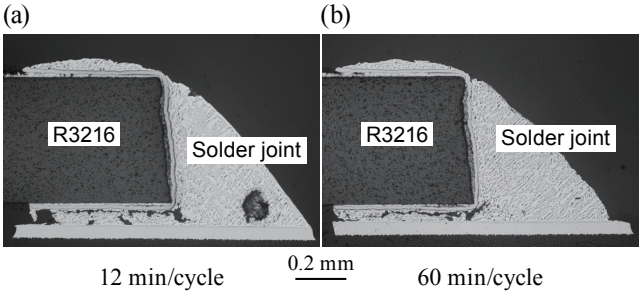

Fig. 14 Cross sections of solder joints after 3000 cycles (−30ºC↔80ºC).

5. Conclusions

In the present study, a novel thermal cycling system capable of the rapid yet uniform heating and cooling of electronic devices for test purposes was fabricated and evaluated. This apparatus is based on the circulation of a shower of air, the temperature of which is controlled. A minimal amount of air at a precisely defined temperature is dispersed homogeneously in the test chamber and moves around the sample. CFD analyses demonstrated that the airflow in this system was as desired. This apparatus has a simple structure allowing the testing of multiple units at the same time while applying identical conditions to each specimen.

Assessments of the temperature distribution of an actual circuit board confirmed that this new system rapidly went to the desired temperature and generated a suitable temperature distribution. The homogeneous, rapid temperature control exhibited by this new system results from the use of a minimal amount of air flowing over the sample.

This work assessed the damage to solder joints resulting from the more rapid thermal cycling applied in the new system. Reducing the cycling period from 60 to 12 min had no significant impact on the fracture mode or crack damage. This new test process is anticipated to have numerous potential applications. These would include thermal cycling of a wide range of materials and electronic components, such as solder joints. Performance tests could be applied under hot or cold conditions and solder reflow could also be performed.

In summary, a temperature cycling apparatus that results in a homogeneous temperature distribution has been developed. This system is anticipated to have applications to power cycling tests involving non-uniform temperature distributions.

References

(1) Taira, S. and Fujino, M., "Studies on Thermal Fatigue Fracture of Metallic Materials", *J. Soc. Mater. Sci. Jpn*, Vol. 25, No. 270 (1976), pp. 218-229.
(2) Toda, H. and Kobayashi M., "Thermal Fatigue Fracture of Materials", *J. Jpn. Inst. Light Met.*, Vol. 59, No. 6 (2009), pp. 312-319.
(3) Kiguchi, S., Nakajima, M., Kurosawa, T. and Sumimoto, H., "Effect of Graphite Morphology and Matrix Structure on Thermal Cycle Fatigue Properties of Cast Iron", *J. JFS* (in Japanese), Vol. 76, No. 1 (2004), pp. 20-25.
(4) Ikuno, H., Iwanaga, S. and Awano, Y., "Thermo-mechanical Fatigue Behavior of Al-Si-Cu-Mg Casting Alloy", *Thermo-mechanical Fatigue Behavior of Materials: Third Volume* (2000), pp. 138-149, *ASTM*.
(5) Ikuno, H., Iwanaga, S. and Awano, Y., "Effect of Porosity on Thermal Fatigue Lives of AC2B Aluminum Alloy Castings", *J. Jpn. Inst. Light Met.* (in Japanese), Vol. 45, No. 11 (1995), pp. 671-676.
(6) Ikuno, H., Iwanaga, S. and Awano, Y., "Development of Simple Thermal Fatigue Test Method Using Low-thermal Expansion Restraining Holders", *J. Soc. Mater. Sci. Jpn.* (in Japanese), Vol. 45, No. 1 (1996), pp. 125-130.
(7) Yamada, H. and Ogawa, K., "Evaluation for Thermal Fatigue Life of Solder Joints in Electronic Components", *R&D Review of Toyota CRDL* (in Japanese), Vol. 31, No. 4 (1996), pp. 43-52.
(8) Sakane, M., "New Challenges for Thermo-mechanical Fatigue, III: Thermo-mechanical Fatigue in Electronic Devices", *J. Soc. Mater. Sci. Jpn.* (in Japanese), Vol. 56, No. 3 (2007), pp. 302-308.
(9) Japan Electronics and Information Technology Industries Association, "Test Method 307B Thermal Shock (Reference Test)", *JEITA Standard No. ED-4701/302: Environmental and Endurance Test Methods for Semiconductor Devices (Stress Test I-2)* (2013), pp. 147-154.
(10) Japan Electronics and Information Technology Industries Association, "Test Method 105A Temperature Cycle", *JEITA Standard No. ED-4701/100A: Environmental and Endurance Test Methods for Semiconductor Devices (Life Test I)* (2013), pp. 35-42.
(11) Patent No. JP2786688 (in Japanese).
(12) Unexamined Patent Pub. H05-267418 (in Japanese).
(13) Unexamined Patent Pub. 2007-333559 (in Japanese).
(14) Tohei, T., Shohji, I., Yoshizawa, K., Nishimoto, M., Kawano, T., Mizutani, Y. and Ohsaki, Y., "Thermal Fatigue Life Evaluation of Lead-free Solder Joint of Chip Size Package with Underfill", *J. Jpn. Inst. Met.* (in Japanese), Vol. 72, No. 3 (2008), pp. 244-248.
(15) Kaga, Y., Yu, Q. and Shiratori, M., "Thermal Fatigue Reliability Estimation for CSP Package Using SDSS and FEA", *J. Jpn. Inst. Electron. Packaging* (in Japanese), Vol. 4, No. 3 (2001), pp. 225-230.
(16) Takahashi, K. and Ogawa, H., "Packaging Technology and Evaluation of Test Method Regarding BGA·CSP for Notebook PCs", *J. Jpn. Inst. Electron. Packaging* (in Japanese), Vol. 1, No. 5 (1998), pp. 364-370.
(17) Nishiura, M., "Comparison between Soldering Property and Mechanical-thermal Fatigue Property of Pb Contained Solder and Sn-Ag-Cu Series Solder Alloy", *J. Jpn. Inst. Electron. Packaging* (in Japanese), Vol. 3, No. 6 (2000), pp. 509-514.

(18) Fukuzono, K., Koide, M. and Watanabe, M., "Efficiency Improvement of Solder Joint Fatigue Life Evaluation for a High-end Pb-free Glass Ceramic BGA Package", *Proc. JIEP Annu. Meet.* (in Japanese), Vol. 24 (2010), pp. 196-197.
(19) Kawada, T., Shioiri, J. and Ueda, T., "Creep of Metals", *OYOBUTURI* (in Japanese), Vol. 24, No. 1 (1955), pp. 18-27.
(20) Nagano, M., Hidaka, N., Watanabe, H., Shimoda, M. and Ono, M., "Effect of Addition Elements on Creep Properties of the Sn-Ag-Cu Lead Free Solder", *J. Jpn. Inst. Electron. Packaging* (in Japanese), Vol. 9, No. 3 (2006), pp. 171-179.
(21) Kawano, K., Naka, Y., Tanie, H., Kimoto, R. and Yamamoto, K., "Fatigue Life Prediction of Solder Joints with the Consideration of High-temperature Degradation", *J. Jpn. Inst. Electron. Packaging* (in Japanese), Vol. 17, No. 2 (2014), pp. 123-131.

Hajime Ikuno
Research Fields:
- Thermal Fatigue Reliability
- Metallic Material

Academic Societies:
- The Japan Institute of Light Metals
- The Japan Institute of Electronics Packaging

Awards:
- R&D 100 Award, 1988
- Light Metal Encouragement Prize, The Japan Institute of Light Metals, 1995
- Technical Development Award, The Society of Materials Science, Japan, 2008